Chemical Engineering Journal 160 (2010) 698–707

Contents lists available at ScienceDirect

Chemical Engineering Journal

journal homepage: www.elsevier.com/locate/cej

# Estimation of alkyd reactors with discrete-delayed measurements☆

Héctor Hernández-Escoto[a,d,*], Teresa López[b,d], Jesús Alvarez[c]

[a] Universidad de Guanajuato, Depto. de Ingeniería Química, Noria Alta s/n, 36050 Guanajuato, Gto., Mexico
[b] Universidad Autónoma Metropolitana – Cuajimalpa, Depto. de Procesos y Tecnología, Artificios 40, 01120 México, D.F., Mexico
[c] Universidad Autónoma Metropolitana – Iztapalapa, Depto. de Ingeniería de Procesos e Hidráulica, Apdo. 55534, 09340 México, D.F., Mexico
[d] Centro de Investigación en Polímeros – Grupo COMEX, 55885 Tepexpan, Edo. de México, Mexico

ARTICLE INFO

*Article history:*
Received 30 December 2009
Received in revised form 23 March 2010
Accepted 23 March 2010

*Keywords:*
Alkyd reactor
On-line monitoring
State estimation
Discrete-delayed measurements

ABSTRACT

This work addresses the problem of designing an on-line dynamic data processor to estimate and predict viscosity, conversion, and molecular weight of an alkyd reactor through discrete-delayed measurements of viscosity. This estimation–prediction scheme is important to monitor, control and stop the batch operation so that its yield is maximized with a product grade within specifications. Since the alkyd polymerization involves a complex reaction of synthetic or natural fatty acids with unknown detailed kinetics, the proposed estimator is designed on the basis of a simple kinetics model with an on-line adjusted observable parameter. The resulting estimator has a systematic construction-tuning procedure coupled with a robust convergence criterion, and its functioning and performance is illustrated with experimental data.



## 1. Introduction

Oil-modified polyesters, commonly called alkyd resins, are important synthetic resins in the surface coating industry because of their low production cost and their convenient utility properties, such as good mechanical and chemical resistance, color retention, gloss, and adherence. The industrial production of alkyd resins is carried out in batch stirred tank reactors where an endothermic condensation-type polymerization of synthetic or natural fatty acids takes place at a constant temperature. The product yield and quality are monitored throughout the course of the reaction by means of discrete-delayed (DD) measurements of conversion and viscosity. These measurements are employed to correct the operation by adding reactants, and to decide when to stop the batch in order to obtain a product within specifications (i.e., conversion and viscosity). In particular, the key decision on the batch termination is taken on the basis of a time-ahead prediction of viscosity, using a preset log–log viscosity–conversion chart in conjunction with the operators' experience. Even though this monitoring–control scheme has been employed in industrial reactors [1], a more efficient and better reactor operation requires, among other aspects: (i) the improvement of existing monitoring and control schemes and their automation, (ii) the development of on-line sensors whose signals can be correlated to conversion and viscosity, and (iii) the development of robust multivariable control schemes to track a prescribed conversion–viscosity nominal trajectory pair.

Regarding the first aspect, this work addresses the on-line estimation and prediction of conversion, viscosity, and molecular weight from the DD measurements of viscosity. As for free-radical polymerization reactors, there are reasonable kinetics models and advanced model-based estimation, control and process design schemes [2]; in the case of alkyd reactors, the treatment of these subjects lags far behind because of the lack of alkyd kinetics understanding and modeling. In fact, the existing alkyd kinetics studies [3–5] report simplified or lumped condensation-type kinetics models which are valid either at low or at high conversion, and this in turn means that the development of industrial monitoring, control and process designs require intensive amounts of laboratory testing, scaling-up and on-line model calibration effort. Thus, the lack of adequate alkyd kinetics models and the DD feature of the viscosity measurement preclude the direct application of the available advanced nonlinear state estimation and control techniques which have been successfully applied to free-radical polymerization reactors; for example, nonlinear geometric observer [6], open-loop-observer [7], extended Kalman filter [8], and Luenberger nonlinear observer [9]. On the other hand, calorimetric estimation techniques for reactors with unknown kinetics [10], the observer-based parameter estimation approach

☆ The first part of this work was done at Centro de Investigación en Polímeros – Grupo COMEX, and the second part was performed at the authors' present affiliations. This paper is based on a preliminary study [13] presented at the IFAC Symposium on Advanced Control of Chemical Processes Advances (ADCHEM), Pisa, Italy, June 14–16, 2000.

* Corresponding author at: Universidad de Guanajuato, Depto. de Ingeniería Química, Noria Alta s/n, 36050 Guanajuato, Gto., Mexico.
Tel.: +52 473 7320006x1424; fax: +52 473 7320006x8139.
*E-mail address:* hhee@quijote.ugto.mx (H. Hernández-Escoto).

1385-8947/$ – see front matter © 2010 Elsevier B.V. All rights reserved.
doi:10.1016/j.cej.2010.03.055

for model consistency assessment [11], the geometric observer approach for continuous plants with sampled measurements [12], and the preliminary work on estimation of alkyd reactors [13], suggest the possibility of addressing the alkyd reactor estimation and time-ahead prediction problem, within a nonlinear geometric estimation framework where the kinetics uncertainty is robustly reconstructed by means of a dynamic observer driven by DD measurements.

In the present work, the alkyd reactor estimation–prediction problem with DD-viscosity measurements is addressed within a nonlinear estimation constructive framework to estimate and time-ahead predict conversion, viscosity and molecular weight on-line. As a further step of the preliminary study [13], the key forecasting issue, and formal convergence considerations assessment are emphasized. The point of departure is a simple third-order reaction rate model whose kinetics constant is regarded as a time-varying parameter that reflects the effect of the unmodeled dynamics. Then, the time-varying nonlinear observability of the conversion-kinetics observability motion is addressed, establishing the robust solvability of the alkyd reactor estimation problem, and yielding the construction and tuning schemes of a nonlinear robustly convergent estimator with time-ahead prediction capability. The robust solvability condition bears physical meaning, the estimator construction is systematic, the gain tuning is visualized and executed with conventional-type notions and guidelines, and the estimator functioning capabilities and limitations are addressed. The functioning and performance of the resulting estimator is shown via experimental data obtained from an industrial reactor.

## 2. The alkyd reactor, and its monitoring and control problem

In an alkyd reactor (Fig. 1), either synthetic or natural fatty acids, polybasic acids, and polyols are polymerized via endothermic reversible complex polyesterification reactions. The reactor is equipped with a condensing–decanting system to remove produced water in order to avoid equilibrium and favor the forward reaction to produce the polymer. The reactor load has a low level of solvent to assist the reaction water withdrawal by dragging the water in an azeotropic solvent–water vapor through the condensing–decanting system, where the water is dropped and the solvent is refluxed to the reactor. The temperature is maintained constant by means of a conventional controller.

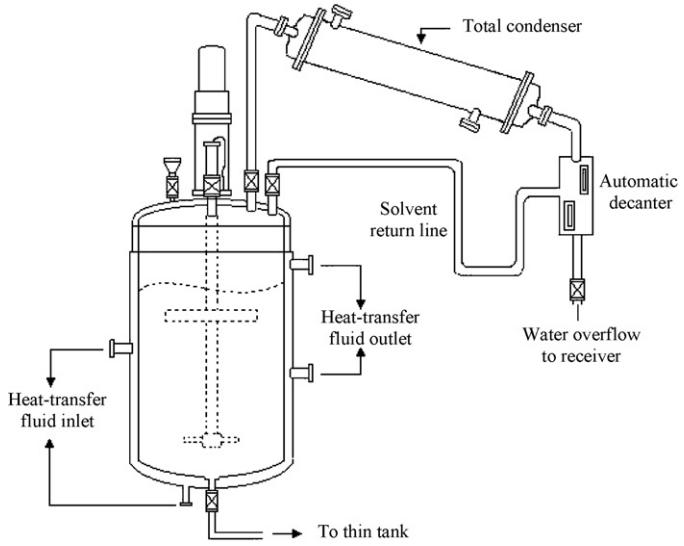


**Fig. 1.** Alkyd reactor.

The key variables that determine the reaction advance and the polymer product quality are conversion of the acid functional group ($c$) (conformed by the fatty and polybasic acids), viscosity ($\nu$), and average molecular weight of the polymer product ($M$). Their monitoring is done on the basis of laboratory analysis of cold-diluted samples, usually taken out at periodic sampling times. The reacting mixture sample is cooled down and diluted because the hot reacting mixture viscosity barely decreases with conversion, and is excessively large for a standard industrial viscometer. In this way, the obtained measurements of conversion ($y_c$) and viscosity ($y_\nu$) are discrete-delayed. Next, a log – log $y_\nu$-vs. – $y_c$ chart is traced and its trajectory (typically linear) is extrapolated to foresee present-time and time-ahead values of $c$ and $\nu$, with the additional assistance of the reactor operator experience. Thus, important operation decisions are made: either (i) to correct the reactor motion by addition of reactants (i.e., a small amount of fatty acids or alcohol) and by manipulating the reactor temperature, or (ii) to stop the reaction at an operator-foreseen conversion that is within specifications, and safely below a critical value associated with the gel point of the cold polymer product. The goal of stopping the reaction close to the cold polymer gel point is to obtain a liquid cold polymer product. Thus, the batch-to-batch operation objective consists in having a sufficiently thin bundle of reactor motions that, with regard to a prescribed nominal operation, is generated by the inexorable presence of load and operation disturbances. The radius of the motion bundle determines the variability of the end product properties.

In order to achieve a more efficient and better batch operation, one must resort to a feedback control; however, the discrete-delayed feature of the measurements, and basing the monitoring scheme on operator experience make it difficult (or not straightforward); meaning that these monitoring features must first be attended. Resorting to an estimation approach, the monitoring problem is translated into one of designing an estimator that, on the basis of a model, and driven by a sequence of DD measurements (i.e., $\{y_\nu(t_0), y_\nu(t_1), \ldots, y_\nu(t_i)\}$) each sampling time instant ($t_i$) on-line yields:

(i) Present-time estimates, at time $t_i$, of conversion $c(t_i)$, viscosity $\nu(t_i)$, and average molecular weight $M(t_i)$.
(ii) Time-ahead predictions, over the future horizon $[t_i,\ t_i+\tau]$ $(0 \le \tau \le t_F - t_i)$, of conversion $c(t_i+\tau)$, viscosity $\nu(t_i+\tau)$, and average molecular weight $M(t_i+\tau)$.

## 3. Reactor and measurement model

Due to the complexity of the polymerization mechanism and raw materials, a detailed kinetics model is lacking, and simple and phenomenological/semi-empirical second, and apparent third-order reaction rate models have been proposed in alkyd kinetics studies [4,5]; however, none of the mentioned reaction rate models apply to the entire course of the reaction, and they only describe the reaction trajectory reasonably well far before the critical gel point. For the purpose at hand, let us recall the empirical relationships typical in the coating industry:

(i) a third-order reaction rate ($r$) model of the acid functional group conversion [4],

$$r = \rho(c,k,c_e); \qquad \rho(c,k,c_e) := k(1-c)(c_e-c)^2, \tag{1a}$$

(ii) a viscosity–conversion expression in a form suggested by the free-volume theory [14],

$$\nu = \mu(c,p_\mu), \qquad \mu(c,p_\mu) := a_\mu e^{b_\mu/(c_\mu - c)}, \qquad P_\mu = [a_\mu, b_\mu, c_\mu]', \tag{1b}$$

(iii) an average molecular weight–conversion relationship [15],

$$M = \eta(c, p_\eta), \qquad \eta(c, p_\eta) := \frac{1 + a_\eta c}{b_\eta + c_\eta c + d_\eta c^2},$$

$$p_\eta = [a_\eta, b_\eta, c_\eta, d_\eta]'; \tag{1c}$$

where the values of the kinetics constant ($k$), and the parameters $c_e$, $p_\mu$ and $p_\eta$ depend on formulation, and must even be recalibrated every certain number of batches for the same formulation. In these proposals, it is ideally assumed that all functional groups of the same type (either acid or basic, but of different raw material) are equally reactive, all functional groups react independently of the chain length, no side reactions occur, and the reaction rates of the elemental reactions are lumped in a global reaction rate.

From a standard kinetics modeling perspective, to force the reaction rate model (1a) to adequately describe the entire course of the reaction, $k$ could be intuitively assumed as a time-varying parameter,

$$k(t) = \kappa(c(t), T(t), w(t)) \tag{2}$$

which depends on reactor variables such as $c$ and $T$, as well as on an unknown number ($n_w$) of unknown ones ($w$) (i.e., those related to the polymer architecture, and/or to diffusion phenomena), in an unknown possibly nonlinear form ($\kappa$).

Through the combination of acid functional groups and heat balances with the relationships (1), taking into account unknown variables and dynamics, and the assumption given by (2) by incorporating the kinetics constant ($k$) and its tendency (v) as dynamical states, and considering the abovementioned monitoring scheme, the following reactor–measurement model is obtained:

$$\dot{c} = r(c, k, c_e), \quad c(t_0) = c_0; \quad y_v(t_i) = \mu(c(t_{i-1}), p_\mu), \quad t_i = t_{i-1} + D \tag{3a}$$

$$\dot{k} = \mathrm{v}, \qquad k(t_0) = k_0; \tag{3b}$$

$$\dot{\mathrm{v}} = a(t), \qquad \mathrm{v}(t_0) = \mathrm{v}_0; \qquad |a(t)| \le \varepsilon_a, \tag{3c}$$

$$\dot{T} = f_T(c, T, k, \mu, p_T), \qquad T(t_0) = T_0; \qquad y_T(t) = T(t), \tag{3d}$$

$$\dot{w} = f_w(c, T, w, k, u, p_w), \quad w(t_0) = w_0; \quad dim\, w = n_w(\text{unknown}); \tag{3e}$$

$$v(t) = \mu(c(t), p_\mu), \qquad M(t) = \eta(c(t), p_\eta), \qquad t \in [t_0, t_F] \tag{3f}$$

where $T$ is the reactor temperature, and $u$ is the system input. In this work, (3d) is called unmodeled $T$-dynamics, and $f_T$ is an unmodeled, possibly nonlinear function with a parameter set $p_T$ that represents the temperature change rate. On the other hand, (3e) is the unknown $w$-dynamics (i.e., $f_w$ is an unknown, possibly nonlinear, function with an unknown parameter set $p_w$, which set the change rate of the unknown states $w$). $v$ and $M$ are the key interest variables. $t_i$ is the sampling time instant, and $D$ is the sampling time; $t_0$ is the initial time (in which the reaction is initiated), and $t_F$ is the scheduled final time in which the reaction is stopped. In this case, $a(t)$ is considered as a bounded input obtained from the second directional derivative of the scalar field $\kappa$ (2) with respect to the vectorial field comprised by the functions $r$, $f_T$ and $f_w$:

$$a(t) := \alpha(c(t), k(t), T(t), w(t), u(t), \dot{u}(t), c_e, p_T, p_w),$$
$$\alpha(c, k, T, w, u, \dot{u}, c_e, p_T, p_w) = L_f^2 \kappa(c, T, w),$$
$$f = [r, f_T, f_w]'$$

Notice that the viscosity measurement ($y_v$) at instant $t_i$ reflects the reactor state at the past instant $t_{i-1}$; and this is the only one proposed for use on-line on the basis of viscosity–conversion (1b); therefore, the on-line conversion measurement could be eliminated, signifying a reduction in costs due to on-line laboratory analysis.

In vector notation, the reactor model (3) is written as follows:

$$\dot{x} = f(x, u(t), p_r) + \pi a(t), x(t_0) = x_0;$$
$$y_v(t_i) = \mu(x(t_{i-1}), p_s), \quad y_T = \pi_T x, \quad t_i = t_{i-1} + D, \tag{4a}$$

$$s(t) = h(x(t), p_s), \quad t \in [t_0, t_F], \quad x = [c, k, \mathrm{v}, T, w]',$$
$$s = [v, M]', \quad p_r[c_e, p_T, p_w]', \quad p_s[p_\mu p_\eta]', \quad f = [r, \mathrm{v}, o, f_T, f_w]',$$
$$h = [\mu, \eta]', \quad \pi = [0, 0, 1, 0, 0]', \quad \pi_T = [0, 0, 0, 1, 0] \tag{4b}$$

Given the continuous differentiability of the map $f$ and that of the input $a(t)$, the initial conditions $x_0$, the input $u$, and the parameters $p_r$ determine a unique reactor state motion,

$$x(t) = \theta_x(t, t_0, x_0, u(\cdot), p_r) \tag{5}$$

## 4. Estimator design

In this section, on the basis of the reactor model (4), the estimator is designed by the straightforward application of the geometric estimation approach of Hernandez and Alvarez [12]. This approach follows a detectability property evaluation of the reactor motion (5) to underlie the construction, tuning, and convergence conditions of the estimator driven by the discrete-delayed viscosity measurement.

### 4.1. Detectability property

According to the indistinguishability-based definition of nonlinear detectability, the reactor motion $x(t)$ (5) is detectable if at each time ($t$) the state ($x$) is uniquely reconstructed from its initial state ($x_0$), the input–output realization $u(t) - y_v(t)$ and its time derivatives. The robust fulfillment of this detectability property implies the possibility of reconstructing the state via a dynamic nonlinear estimator.

For the moment, it is assumed that the viscosity measurement is continuous–instantaneous, and that $f_T$ and $f_w$ are known, in the understanding that these (methodologic) unrealistic assumptions will be removed later. Physically speaking, the reactor detectability property amounts to the solvability of the following differential estimation problem: the reconstruction of the reactor motion $x(t)$ (5) and the trajectory $s(t)$ (4b) on the basis of the data,

$$DS = \{x_0, y_a(t), p\}, \qquad y_a = [y_v, \dot{y}_v, \ddot{y}_v]', \qquad p = [p_r, p_s]' \tag{6}$$

To solve this problem, the viscosity measurement Eq. (4a) is recalled in its continuous–instantaneous version, $y_v(t) = \mu(c(t), p_s)$; next, two successive time-derivatives are taken by replacing the resulting time-derivatives $\dot{c}$ and $\dot{k}$ (on the right-hand side) by the map $r(c, k, c_e)$ and v ((3a) and (3b)), respectively; finally the $T$ and $w$ dynamics ((3d) and (3e)), as well as the relationship $s$-vs.-$x$ (4b) are recalled, and the following differential–algebraic system is obtained:

$$\phi(x_c(t), p_e) = y_a(t), \qquad x_c = [c, k, \mathrm{v}]', \qquad p_e = [c_e, p_\mu]', \tag{7a}$$

$$\dot{x}_u = f_u(x_c, x_u, p_r), \qquad x_u(t_0) = x_0^u, \qquad x_u = [T, w]',$$
$$f_u = [f_T, f_w]', \qquad x = [x_c, x_u]', \tag{7b}$$

$$s(t) = h(x_c(t), p_s), \tag{7c}$$

where $x_c$ refers to the kinetics state set, and $x_u$ to the unmodeled state set. It can be observed that in the cascade interconnection between the algebraic part and the differential one, the nonlinear

map vector $\phi$ (A.1) does not depend on the unknown exogenous input $a(t)$, and the key interest variable set ($s$) does only depend on $x_c$.

Since the Jacobian matrix of $\phi$, $J(x_c, p_e)$ (A.2), is nonsingular along any kinetics motion $x_c(t)$ before the total conversion because the kinetics motion $x_c(t)$ is bounded ($x_c$: $0 \le c \le 1$, $0 \le k \le \varepsilon_k$, $0 \le \mathrm{v} \le \varepsilon_\mathrm{v}$) by inherent physical limitations, the three-equation algebraic system (7a) admits, at each time $t$, a unique and robust solution for $x_c$,

$$x_c = \sigma(y_a, p_e) \tag{8}$$

Next, the following differential estimator, driven by the output measurements $y_a$ and the input signals $u$, is obtained by the substitution of expression (8) into system (7):

$$x_c(t) = \sigma(y_a(t), p_e), \tag{9a}$$

$$\dot{x}_u = f_u^*(x_u, y_a(t), u(t), p_r), \qquad x_u(t_0) = x_0^u,$$
$$f_u^*(x_u, y_a, u, p_r) = f_u(x_u, \sigma(y_a, p_e), u, p_r) \tag{9b}$$

$$s(t) = h^*(y_a(t), p_e, p_\eta), \qquad h^*(y_a, p_e, p_\eta) = h(\sigma(y_a, p_e), p_\eta) \tag{9c}$$

Additionally, the ($\infty$-norm) condition number (a $\infty$-norm is considered for understanding purposes),

$$C_J \approx \frac{1}{[\partial_k r(c, c_e)]} \tag{10a}$$

of $J(x_c, p_e)$ varies along any reactor motion according to the following expressions:

$$C_J \to c_e^2 \ \text{ as } \ c \to 0, \quad \text{and} \quad C_J \to \infty \ \text{ as } \ c \to 1, \tag{10b}$$

Analyzing the differential estimator (9) on the framework of the detectability notion given in [12], the next conclusions follow: (i) the observability matrix $J(x_c, p_e)$ and its non-singularity establish that the reactor motion $x(t)$ (5) is robustly partially observable with observability index $\kappa_o = 3$, and (ii) the differential equation (9b) is the unobservable dynamics whose unique solution is the unobservable motion,

$$x_u(t) = \theta_u(t, t_0, x_0^u, y_a(\cdot), u(\cdot), p_r), \tag{11}$$

From heat and mass capacity and conservation arguments, as well as kinetics considerations in conjunction with the semi-batch nature of the reactor, the unobservable motion $x_u(t)$ (11) is robust with respect to errors in the estimator data set $DS$ (6), in the sense that: (i) arbitrarily small estimate errors can be obtained by making the data errors sufficiently small; and (ii) the estimation errors grow slowly with time and remain bounded. Notice that, through the condition number value (10), the solvability robustness is good at the beginning of the reaction, later breaks down as the reaction continues, and becomes poor when total conversion is approached. It is hoped the observability property is reasonably robust and conditioned in the critical period before the gel point (close to the total conversion) where the estimation–prediction values are most needed.

The robustness of the partial observability property (given by (10)), and the bounded data-bounded state error property of the unobservable motion $x_u(t)$ (11) imply the robust detectability of any reactor motion $x(t)$, and this in turn implies: (i) the possibility of reconstructing the reactor motion $x(t)$ and the trajectory $s(t)$ via a robust dynamic estimator with adjustable convergence rate for the observable state $x_c$ and with unobservable dynamics-fixed convergence rate for the unobservable state $x_u$; (ii) the differential estimator (9) constitutes the limiting behavior attainable with any estimator; and (iii) $x_c$ and $s$ can be reconstructed without $x_u$. Finally, it must be pointed out that this robust detectability assessment and its implications are valid for any possible motion in the entire class of alkyd reactors.

### 4.2. Estimator construction

Recalling that the interest variables are $c$, $\nu$ and $M$, and that they only depend on the kinetics state set $x_c = [c, k, \mathrm{v}]'$, towards estimator construction on the basis of the reactor model (3), the detectability property characterization involves considering $a(t)$ equal to zero, and dropping the unobservable dynamics ((3d) and (3e)). Next, the estimator construction followed a straightforward application of the construction procedure given in [12] with two tenuous modifications:

(i) The estimation sequence was delayed in one-step by replacing the discrete-instantaneous output estimation error $\{y(t_i) - \mu(c(t_i),\ p_\mu)\}$ with the DD one $\{y(t_i) - \mu(c(t_{i-1}),\ p_\mu)\}$, and considering the interval $[t_{i-1}, t_i]$, instead of $[t_i, t_{i+1}]$, as the "work" one.
(ii) A time-ahead prediction operator (the reactor model with $a(t) = 0$, and without $T$ and $w$ dynamics, initialized at the present time estimate) was appended.

In this way, the estimator is given by:

$$\hat{c}(t_i) = \theta_c(t_i, t_{i-1}, \hat{c}(t_{i-1}), \hat{k}(\cdot), \hat{p}_e) + G_c(\hat{c}(t_{i-1}), \hat{p}_e, D, \xi, \omega)(y(t_i) - \mu(\hat{c}(t_{i-1}), \hat{p}_e)), \qquad \hat{c}(t_0) \approx c(t_0) \tag{12a}$$

$$\hat{k}(t_i) = \hat{k}(t_{i-1}) + D\,\hat{\mathrm{v}}(t_{i-1}) + G_k(\hat{c}(t_{i-1}), \hat{k}(\cdot), \hat{p}_e, D, \xi, \omega)(y(t_i) - \mu(\hat{c}(t_{i-1}), \hat{p}_e)), \qquad \hat{k}(t_i) \approx k(t_0) \tag{12b}$$

$$\hat{\mathrm{v}}(t_i) = \hat{\mathrm{v}}(t_{i-1}) + G_\nu(\hat{c}(t_{i-1}), \hat{k}(t_{i-1}), \hat{\mathrm{v}}(t_{i-1}), \hat{p}_e, D, \xi, \omega)(y(t_i) - \mu(\hat{c}(t_{i-1}), \hat{p}_e)), \qquad \hat{\mathrm{v}}(t_0) = 0 \tag{12c}$$

$$\hat{c}(t) = \theta_c(t_t, t_i, \hat{c}(t_i), \hat{k}(\cdot), \hat{p}_e),$$
$$\hat{k}(t) = \hat{k}(t_i) + (t - t_i)\hat{\mathrm{v}}(t_i), \qquad \hat{\mathrm{v}}(t) = \hat{\mathrm{v}}(t_i) \tag{12d}$$

$$\hat{\mathrm{v}}(t) = \mu(\hat{c}(t), \hat{p}_e),$$
$$\hat{M}(t) = \eta(\hat{c}(t), \hat{p}_e), \qquad t \in [t_i, t_F^*), \qquad t_i = t_{i-1} + D \tag{12e}$$

where $\hat{z}$ denotes the estimate of the variable $z$, $\theta_c$ is the transition map of the differential equation, $\dot{c} = r(c, k, c_e)$, $c(t_0) = c_0$, yielding $c(t) = \theta_c(t, t_0, c_0, k(\cdot), c_e)$; and the maps $\mu$ and $\eta$ are defined in Eqs. (1b) and (1c). $G_c$, $G_k$ and $G_\nu$ (defined in Appendix A) are nonlinear gains constructed on the basis of the observability matrix, $J(x_c, p_e)^{-1}$ (A.2), which depend on the state, a tuning parameter pair ($\xi$, $\omega$) and the sampling-delay time ($D$). The tuning parameter pair ($\xi$, $\omega$) is chosen in such a way to have stable viscosity estimation error dynamics ($\varepsilon = \hat{y} - y$) (the coefficients $\bar{g}_1$, $\bar{g}_2$ and $\bar{g}_3$ are defined in Appendix A),

$$\varepsilon(t_{i+3}) + \bar{g}_1(\xi, \omega, D)\varepsilon(t_{i+2}) + \bar{g}_2(\xi, \omega, D)\varepsilon(t_{i+1}) + \bar{g}_3(\xi, \omega, D)\varepsilon(t_i) = q_y \approx 0, \tag{13}$$

which is quasi-linear, non-interactive and pole-assignable (qLNPA). $\xi$ and $\omega$ are the damping factor and the characteristic frequency of this dynamics, respectively; and $q_y$ accounts for the nonlinearities that potentially destabilize the dynamics. Due to the qLNPA feature of the underlying output error dynamics (13), the tuning of the adjustable parameter pair ($\xi$, $\omega$) and the choice (if it was possible) of the sampling-delay time ($D$) can be executed with the standard techniques and notions employed in the conventional-type design of single-input controllers and single measurement

filters [16], establishing a clear relationship between the choice of $\xi$, $\omega$ and $D$, and the kind of estimation error response.

From the estimator structure, the first part, constituted by (12a)–(12c) and (12e), is visualized as a closed loop-observer that yields the estimate sequences $\{\hat{c}(t_i)\}$, $\{\hat{k}(t_i)\}$, $\{\hat{v}(t_i)\}$, $\{\hat{\nu}(t_i)\}$ and $\{\hat{M}(t_i)\}$ ($i=0,1,2,\ldots$) convergent to the current sequences $\{c(t_i)\}$, $\{k(t_i)\}$, $\{v(t_i)\}$, $\{\nu(t_i)\}$ and $\{M(t_i)\}$, respectively; and the second part, constituted by (12d) and (12e), is visualized as an open-loop-observer that yields, at each sampling time instant, the predictions $\hat{c}(t_i+\tau)$, $\hat{k}(t_i+\tau)$, $\hat{v}(t_i+\tau)$, $\hat{\nu}(t_i+\tau)$, and $\hat{M}(t_i+\tau)$ that approximate the actual values of $c(t_i+\tau)$, $k(t_i+\tau)$, $v(t_i+\tau)$, $\hat{\nu}(t_i+\tau)$ and $M(t_i+\tau)$, respectively, over a horizon time $t_i+\tau<t_F^*$ ($t_F^*$ is the ultimate value that can take the batch time).

### 4.3. Estimator convergence

In this section, the estimator convergence criteria are stated and interpreted, and the main technical arguments are provided in Appendices B and C.

It is considered that the viscometric observer (12) is run with an approximated data set (see (6)),

$$\hat{DS}=\{\hat{x}_{c_0},\hat{y}_a,\hat{p}_e\};\qquad \hat{x}_{c_0}=x_{c_0}+e_{c_0},$$

$$\hat{y}_a=y_a+e_a,\qquad \hat{p}_e=p_e+e_{p_e},$$

whose errors are bounded,

$$|e_{c_0}|\le\delta_{x_0},\qquad |e_a|\le\delta_y,\qquad |e_{p_e}|\le\delta_p.$$

On the basis of the output viscosity estimation error dynamics (13), an overshoot factor ($a_0$) due to initial estimation error ($e_{c_0}$), and a Lipschitz constant ($L$) from the nonlinearities enclosed on $q_y$, are identified. $L$ represents the sensitivity of the estimator through the nonlinear map $q_y$ with respect to the estimation errors ($e_c$). As explained in Appendix B, the viscometric estimator yields convergent (present time) estimates of $c$, $k$, v, $\nu$ and $M$ if:

(i) the sampling time is chosen below an upper limit $D^+$ that is set by $a_oL$:

$$D\le D^+(a_oL);\quad \text{where}\quad \partial_{a_oL}D^+<0 \tag{14a}$$

(ii) once the damping factor $\xi$ is set sufficiently large (i.e., $\xi=0.71$), the characteristic frequency $\omega$ is chosen within an interval ($\omega^-$, $\omega^+$) determined by $a_oL$ and $D$:

$$\omega^-(a_oL,D)<\omega<\omega^+(a_oL,D);$$

$$\partial_{a_oL\,\text{or}\,D}\omega^->0,\qquad \partial_{a_oM\,\text{or}\,D}\omega^+<0 \tag{14b}$$

According to Condition (i), perturbations in measurement, modeling errors and model nonlinearities impose, through $L$, an upper limit $D^+$ for the admissible choices of the sampling-delay time $D$, and such limit is small when $L$ is large. Condition (ii) says that modeling errors and model nonlinearities (through $L$), and the loss of information (through $D$) impose a bounded from below and above interval ($\omega^-$, $\omega^+$) of admissible $\omega$ values, and that the ($\omega^-$, $\omega^+$)-interval size is small when $D$ or $L$ is large. In fact, there is a value $\omega=\omega^*$ in the ($\omega^-$, $\omega^+$)-interval where the estimation convergence rate is maximum, and when $D=D^+$, the ($\omega^-$, $\omega^+$)-interval collapses into the point $\omega^*$.

With respect to the open-loop convergence for (12d), from the reactor model (3a)–(3c), the following statements can be drawn:

(i) the conversion motion is uniformly stable since $\partial_c r(c,k,c_e)<0$ for the entire reaction course, and its prediction error is uniformly bounded as follows:

$$|\hat{c}(t_i+\tau)-c(t_i+\tau)|\le\lambda_c|\hat{c}(t_i)-c(t_i)|,\quad \lambda_c>0. \tag{15a}$$

(ii) the motions $k(t)$ and $v(t)$ potentially grow and are not asymptotically stable. However, from batch capacity arguments and kinetics considerations, it can be said that their prediction errors remain bounded, during the batch operation as follows:

$$|\hat{k}(t_i+\tau)-k(t_i+\tau)|\le\varepsilon_k^*(t_F^*-t_i),\qquad \varepsilon_k^*(t_F^*-t_i)\le\varepsilon_k, \tag{15b}$$

$$|\hat{v}(t_i+\tau)-v(t_i+\tau)|\le\varepsilon_v^*(t_F^*-t_i),\qquad \varepsilon_v^*(t_F^*-t_i)\le\varepsilon_v. \tag{15c}$$

Despite the non-asymptotic convergence of $k$ and $\nu$ predictions, the $c$-prediction is convergent, and since $\nu$ and $M$ only depend on $c$, it can be said that the prediction of these, through (12e), will be convergent. It can be observed that the performance of $c$-prediction depends on the updated $c$-estimate each sampling instant ($t_i$), and that the prediction error of $c$ is directly proportional to the estimation error of $c$ (15a): if the $c$-estimate error decays every sampling instant, the $c$-prediction error, starting at every sampling instant, will be smaller over the time horizon $\tau$, and therefore the predictions on viscosity and molecular weight will also be.

Typically the size of the sampling time-interval $D$ is fixed by the monitoring procedures, and the damping factor is set sufficiently large (i.e., $\xi=0.71$), with the characteristic frequency $\omega$ remaining as the unique tuning parameter. However, considering that there is sometimes some freedom in setting $D$, from the above facts on estimator convergence, the following tuning guidelines can be dictated:

(i) If there is a large uncertainty in the model parameters $c_e$, $p_\mu$ and $p_\eta$, start choosing the smallest $D$ possible.
(ii) Fix $\xi$ sufficiently large (i.e., 0.71), test the estimator with a large gain $\omega$ (i.e., the dead-beat $\omega=0.333D$); if non-convergence is obtained, decrease the $\omega$ value. Once convergence is observed, decrease and increase $\omega$ to determine the ($\omega^-$, $\omega^+$) interval, and the optimum $\omega$ value for convergence rate. Try with larger $\xi$'s. If there is non-convergence, it means that the size of the sampling time is longer than the maximum allowed by $L$.
(iii) If the estimator performance observed is good, consideration can be given to increasing sampling time, repeating step (ii), until finding a convenient size for $D$, and determining $D^+$.

It must be pointed out that if $L$ was quantitatively known, the optimum choice of $D$ and $\omega$ would be easy. However, its determination goes beyond the scope of this work.

## 5. Implementation

### 5.1. Experimental setting and testing motion behavior

To test the performance of the proposed estimator, an experimental alkyd polymerization of fatty acids, phtalic anhydride, glycerine, and pentaeritritol was considered [13]. The case presents an operation carried out at constant temperature, at the end of the reaction (from $c=0.794$ up to the batch end). Every 20 min a reacting mixture sample was taken out, cooled, diluted and analyzed to obtain viscosity, acid functional group conversion and polymer average molecular weight, and this involved an analysis-delay time of 20 min ($D=20$ min). The viscosity measurements are fed off-line to the estimator in the understanding that the other measurements of conversion and molecular weight are only used for comparison purposes. From a nonlinear regression fitting over a set of experimental runs [13] (at the end of reaction courses), the following viscosity and average molecular weight parameters (see (1b) and (1c)) were obtained:

$$p_\mu=[a_\mu,b_\mu,c_\mu]'=[16.00433,0.10493,1.01388]'$$

$$p_{\eta=}[a_\eta,b_\eta,c_\eta,d_\eta]'=[-0.32481,0.00536,-0,00561,0.00032]'$$

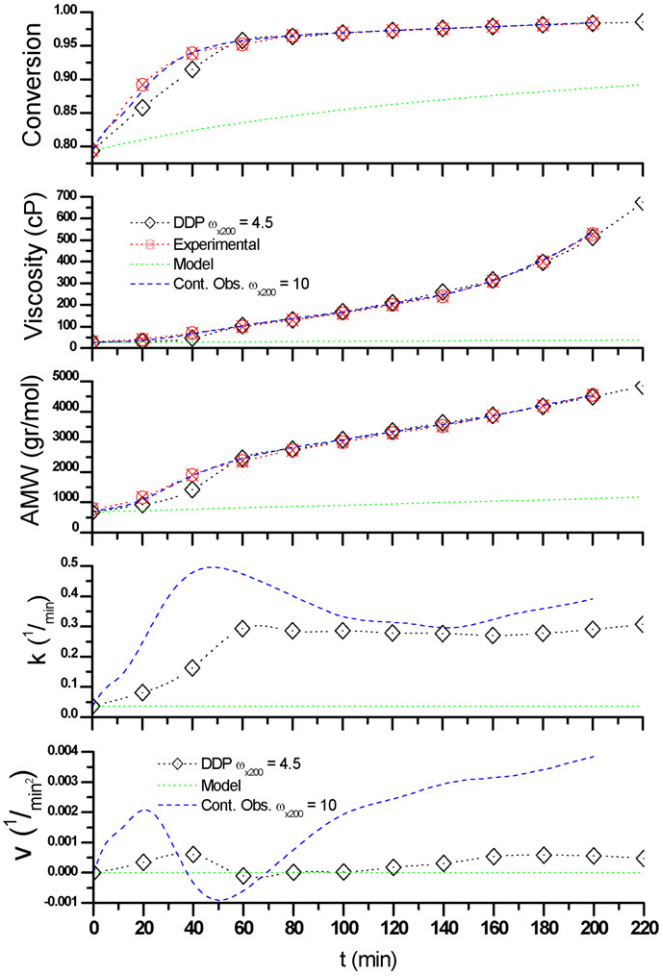


**Fig. 2.** Performance for (present-time) estimates: ($D$, $\omega_{\times 200}$) = (20 min, 4.5).

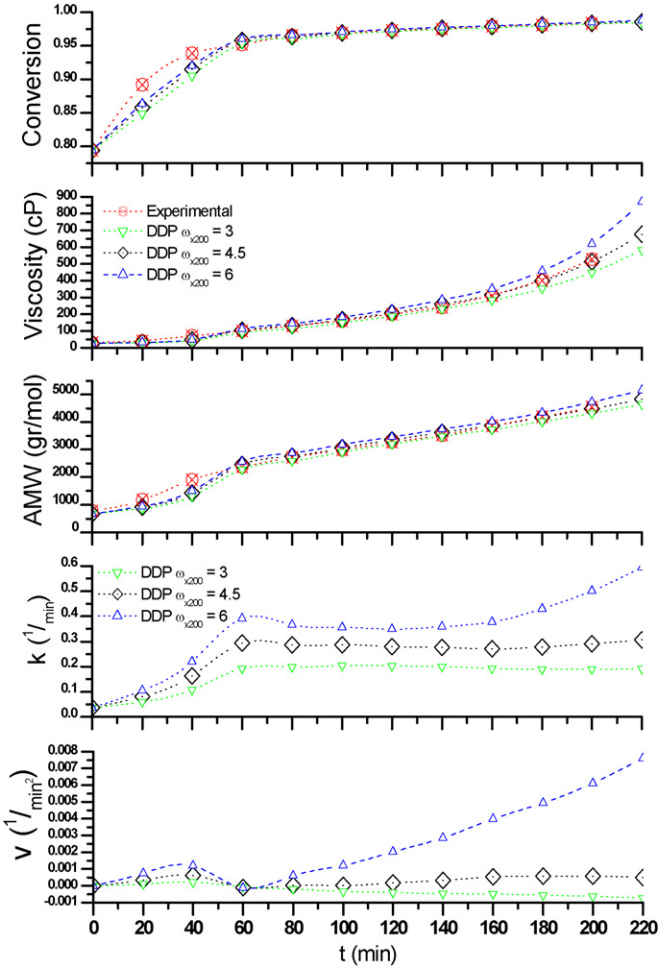


**Fig. 3.** Performance for present-time estimates ($D$ = 20 min): (···▽···) $\omega_{\times 200}$ = 3, (···◊···) $\omega_{\times 200}$ = 4.5, (–△–) $\omega_{\times 200}$ = 6.

The kinetic parameter $c_e$ was set to 1.1358. These parameter values are similar to the ones reported in [13].

### 5.2. Estimator functioning

For the estimator, the initial conversion was set approximately equal to the actual conversion ($c_0$ = 0.794). To set the initial value of the reaction rate parameter, its rigorous definition $k = k^* A_0^2$ was recalled, where 1317.6 $\text{min}^{-1} \times (\text{acid equivalent unit/g})^{-2}$ is a typical value for $k^*$ [4], and for $A_0$, the initial concentration of acid equivalents (0.005276 acid equivalent unit/g). Thus, the initial reaction rate parameter was set to $k_0$ = 0.0367 $\text{min}^{-1}$. The time-derivative of the reaction rate parameter was set to $v_0 = 0$. The tuning parameter $\omega$ was found at 4.5/200 to obtain the best estimator performance.

The experimental data (⊠), the present-time estimates (◊), and the non-adjusted model prediction (···) are shown in Fig. 2, where DDP (discrete data processor) refers to the performance of the estimator (predictor + corrector). Assuming a frequent ($D$ = 0.5 min) measurement obtained from a regression of the experimental data, frequent estimates (Continuous Observer (---)) are also shown for comparison purposes, in the understanding that this performance is similar to a continuous-measurement estimator. The estimates converge adequately (beginning at the 3rd step, at 60 min), and performance is comparable with the frequent estimates that almost exactly track the conversion, viscosity and molecular weight motions. With regard to the reaction rate parameter ($k$) and its time-derivative (v), their estimates do not track those of the frequent estimates; however, it could be said that the reaction rate parameter has been sufficiently adjusted to yield good performance, though not at the end. Its effect can be observed at the end of the viscosity trajectory (close to the gel point) where the estimates seem to come slightly unstuck. With respect to the conversion ($c$), it can be observed that the estimation error of the frequent estimates and the discrete estimates cannot be distinguished; however, in the viscosity trajectory this difference in convergence can be distinguished, because small variations in conversion yield large variations in viscosity, and this large variation is stressed close to the gel point, at the trajectory end.

To obtain the best present-time estimate, several runs were made scanning the tuning parameter $\omega_{\times 200}$ from 1 up to 8. In Fig. 3, estimates for $\omega_{\times 200}$ = 3 (▽), 4.5 (◊) and 6 (Δ) are shown and compared with the experimental data (⊠). The first value corresponds to the "threshold" of convergence; lower values do not yield convergent estimates. As the $\omega_{\times 200}$ value is increased, performance improves. However, after $\omega_{\times 200}$ = 4.5, performance decreases. Thus, $\omega_{\times 200}$ = 6 corresponds to the "threshold" of non-convergence; greater values do not yield convergent estimates. This corroborates the lower and upper limits for the tuning parameter $\omega$ predicted by Condition (ii) of convergence.

In Figs. 4–6, the time-ahead predictions are shown, starting in each sampling instant. Remember that time-ahead prediction performance depends on the adequate updating of the state estimates (each sampling time). In Fig. 4, predictions starting from the initial

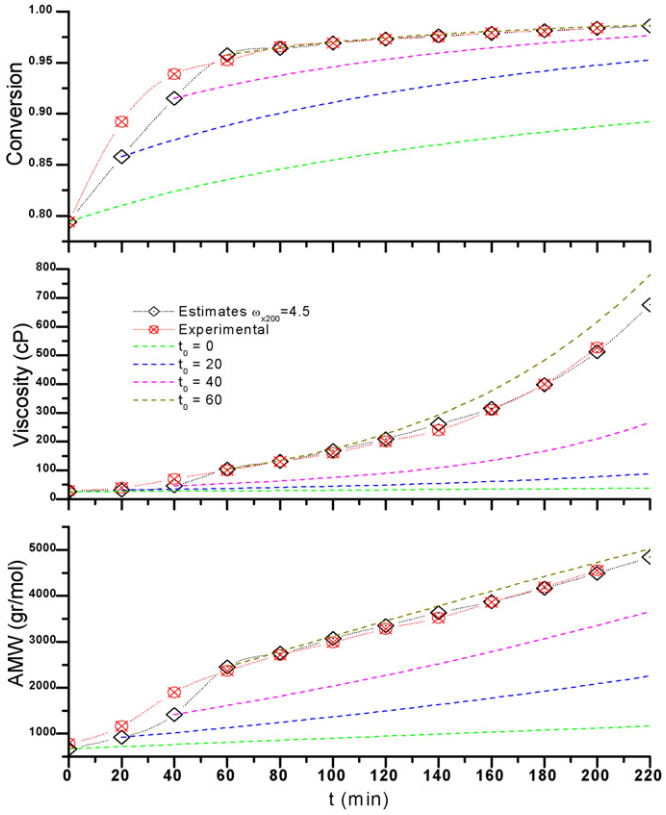


**Fig. 4.** Performance for (time-ahead) predictions. First steps ($t_0$ = 0, 20, 40, 60 min).

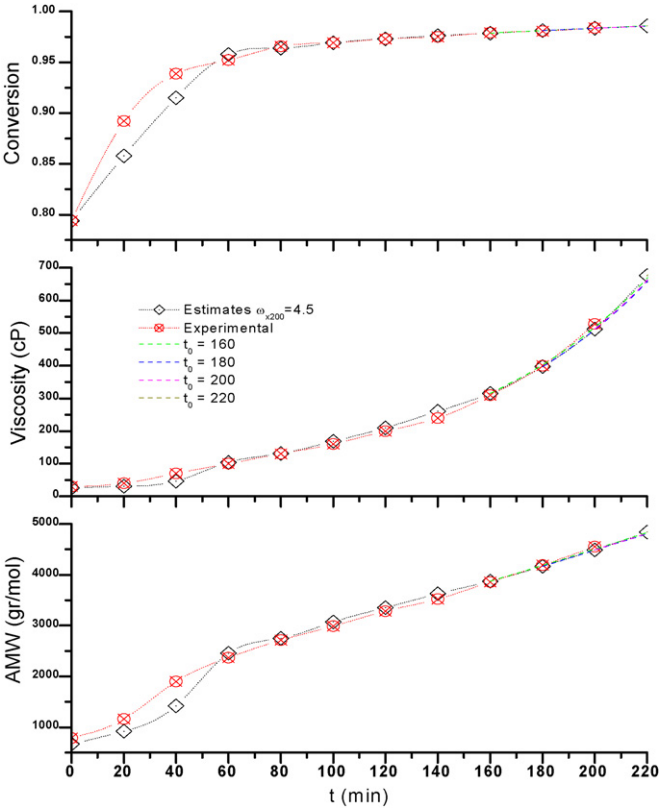


**Fig. 6.** Performance for (time-ahead) predictions. Final steps ($t_0$ = 160, 180, 200, 220 min).

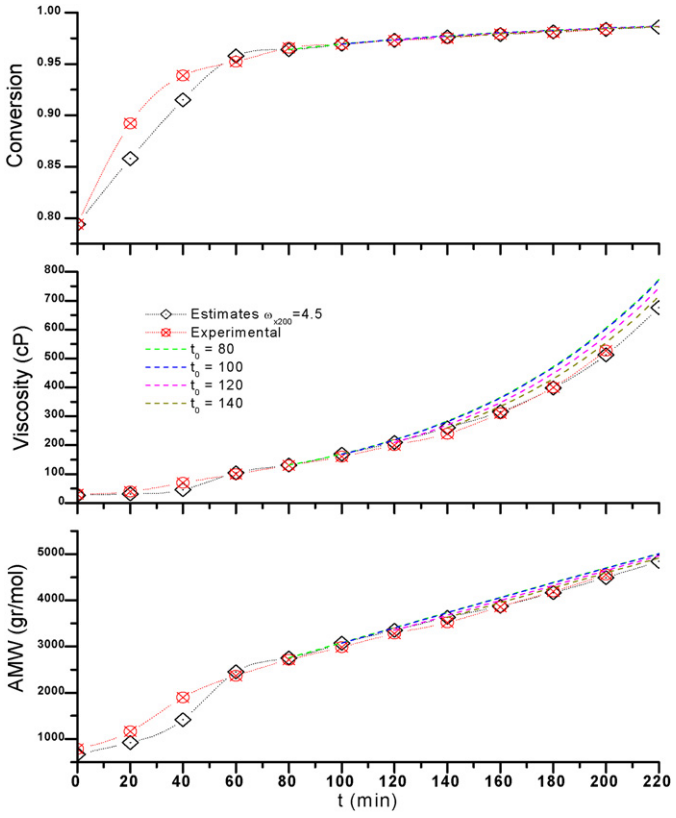


**Fig. 5.** Performance for (time-ahead) predictions. Intermediate steps ($t_0$ = 80, 100, 140 min).

and the first three steps ($t_i$ = 0, 20, 40, 60 min) are shown. For $t$ = 0, 20 and 40 min, the performance is inadequate. However, once the present-time estimates converge (at $t$ = 60 min), one can say that the conversion is adequately updated and the reaction rate parameter and its time-derivative are sufficiently adjusted to yield a good time-ahead prediction. In Fig. 5, time-ahead predictions starting from intermediate steps ($t_i$ = 80, 100, 120, 140) are shown. It can be observed that the predictions obtained have sufficient information to predict the time at which the gel point will be reached. Finally, in Fig. 6, predictions starting from final steps ($t_i$ = 160, 180, 200, 220) are shown. At these times, the estimates have good convergence, implying a good time-ahead prediction.

## 6. Conclusions

For a class of batch alkyd reactors with discrete-delayed viscosity measurements, an industrially oriented robust nonlinear estimator was designed to present-time estimate and to time-ahead predict the key variables related to production rate and product quality. The uncertain kinetic model used led to an on-line estimation or adjustment of the reaction rate parameter. Following a geometric estimation approach, the estimator was systematically constructed and tuned, and corresponding robust convergence criteria were obtained. The functioning of the estimator was tested with industrial-scale experimental data. The performance obtained is quite acceptable and corroborates the theoretical convergence findings. Moreover, the information on the evolution of a reaction rate parameter provides valuable on-line information and insight into the complex alkyd kinetics. In principle, the performance of the estimator can be improved by using a more refined reactor-measurement model. Finally, the proposed estimator could be used to design a discrete-time controller to track a prescribed nominal operation.

## Appendix A. Nonlinear maps and gains

- Observability map (the maps $r$ and $\mu$ are defined in (1a) and (1b), respectively):

$$\phi(x_c, p_e) = [\phi_c(x_c, p_e), \phi_k(x_c, p_e), \phi_v(x_c, p_e)]',$$
$$x_c = [c, k, v]', \qquad p_e = [c_e, p_\mu]' \tag{A.1}$$

where $(\partial_x f = \partial f/\partial x)$
$\phi_c(x_c, p_e) = \mu(c, p_\mu), \qquad \phi_k(x_c, p_e) = \partial_c \mu(c, p_\mu) r(c, k, c_e)$
$\phi_v(x_c, p_e) = \partial^2_{c_2} \mu(c, p_\mu) r(c, k, c_e)^2 + \partial_c \mu(c, p_\mu)(\partial_c r(c, k, c_e) r(c, k, c_e) + \partial_k r(c, c_e) v)$

- Observability matrix ($J(x_c, p_e) = \partial_{x_c} \phi(x_c, p_e)$):

$$J(x_c, p_e) = \begin{bmatrix} J_{11}(x_c, p_e) & 0 & 0 \\ J_{21}(x_c, p_e) & J_{22}(x_c, p_e) & 0 \\ J_{31}(x_c, p_e) & J_{32}(x_c, p_e) & J_{33}(x_c, p_e) \end{bmatrix} \tag{A.2}$$

where

$$J_{11}(x_c, p_e) = \partial_c \phi_k(x_c, p_e)$$

$$J_{21}(x_c, p_e) = \partial_c \phi_k(x_c, p_e), \qquad J_{22}(x_c, p_e) = \partial_k \phi_k(x_c, p_e)$$

$$J_{31}(x_c, p_e) = \partial_c \phi_v(x_c, p_e), \qquad J_{32}(x_c, p_e) = \partial_k \phi_v(x_c, p_e),$$
$$J_{33}(x_c, p_e) = \partial_v \phi_v(x_c, p_e)$$

- Nonlinear gains:

$$G(x_c, p_e, D, \xi, \omega) = [G_c, G_k, G_v]' = [J(x_c, p_e)^{-1}][\Omega(D)][g(D, \xi, \omega)] \tag{A.3a}$$

where

$$\Omega(D) = \begin{bmatrix} 1 & D & 1/2D^2 \\ 0 & 1 & D \\ 0 & 0 & 1 \end{bmatrix},$$

$$g(D, \xi, \omega) = [g_1(D, \xi, \omega), g_2(D, \xi, \omega), g_3(D, \xi, \omega)]' \tag{A.3b,c}$$

$$g_1(D, \xi, \omega) = 3 - 2e^{\xi\varpi}\cos(\zeta\varpi) - e^{\varpi},$$
$$\zeta = \sqrt{1 - \xi^2}, \qquad \varpi = -D\omega \tag{A.3d,e,f}$$

$$g_2(D, \xi, \omega) = \frac{1}{2D}(3g_1(D, \xi, \omega) - 4 + e^{2\xi\varpi} + 2e^{(\xi+1)\varpi}\cos(\zeta\varpi) + e^{(2\xi+1)\varpi}) \tag{A.3g}$$

$$g_3(D, \xi, \omega) = \frac{1}{D^2}(g_1(D, \xi, \omega) - 2 + e^{2\xi\varpi} + 2e^{(\xi+1)\varpi}\cos(\zeta\varpi) - e^{(2\zeta+1)\varpi}) \tag{A.3h}$$

- Coefficients of the output estimation error dynamics (13):

$$\bar{g}_1(\xi, \omega, D) = g_1(D, \xi, \omega) - 3 \tag{A.4a}$$

$$\bar{g}_2(\xi, \omega, D) = 3 - 2g_1(D, \xi, \omega) + Dg_2(D, \xi, \omega) + D^2 g_3(D, \xi, \omega) \tag{A.4b}$$

$$\bar{g}_3(\xi, \omega, D) = (1/2)D^2 g_3(D, \xi, \omega) - Dg_2(D, \xi, \omega) + g_1(D, \xi, \omega) - 1 \tag{A.4c}$$

## Appendix B. Proof for convergence conditions of present-time estimates

Recall the estimator part that yields the present-time estimates (12a)–(12c), and rewrite it in its compact vector notation,

$$\hat{x}_c(t_i) = \theta(t_i, t_{i-1}, \hat{x}_c(t_{i-1}), \hat{p}_e) + G(\hat{x}_c(t_{i-1}), \hat{p}_e, D, \xi, \omega)(y_v(t_i) - \mu(t_{i-1})),$$
$$\psi(t_i) = \mu(t_{i-1}), \tag{B.1a}$$

$$\hat{v}(t_i) = \mu(\hat{x}_c(t_{i-1}), \hat{p}_\mu), \qquad \hat{M}(t_i) = \eta(\hat{x}_c(t_{i-1}), \hat{p}_\eta). \tag{B.1b}$$

Consider the coordinate change $z = \phi(x_c, p_e)$ associated with the detectability property (7), and apply it to the reactor model (4a) and to the estimator (B.1), to take them into the following normal discrete-time form:

$$z(t_{i+1}) = \Omega(D)z(t_i) + \int_{t_i}^{t_{i+1}} .\Omega(t_{i+1}) - \tau)\pi\,\varphi(z(\tau), \alpha(\tau), p_e)d\tau, \tag{B.2a}$$

$$v(t_i) = \delta z(t_i), \qquad M(t_i) = \eta^*(z(t_i), p_e, p_\eta). \tag{B.2b}$$

$$\zeta(t_{i+1}) = \Omega(D)\zeta(t_i) + \int_{t_i}^{t_{i+1}} .\Omega(t_{i+1} - \tau)\pi\,\varphi(\zeta(\tau), (\hat{\alpha} = 0), \hat{p}_e)d\tau + g(D, \xi, \omega)\delta(z(t_i) - \zeta(t_i)), \tag{B.3a}$$

$$\hat{v}(t_i) = \delta\zeta(t_i), \qquad \hat{M}(t_i) = \eta^*(\zeta(t_i), \hat{p}_e, \hat{p}_\eta). \tag{B.3b}$$

where

$y_v(t_{i+1}) = v(t_i) = \mu(c(t_i), p_\mu) = \delta z(t_i), \qquad \pi = [0, 0, 1]'; \qquad \delta = [1, 0, 0],$
$\varphi(z, \alpha, p_e) = [(\partial_c \phi_v)(r) + (\partial_k \phi_v)(v) + (\partial_v \phi_v)(\alpha)]_{/z=\phi^{-1}(c,k,v),}$
$\eta^*(z(t_i), p_e, p_\eta) = \eta(x_c(t_i), p_\eta)_{/x=\phi^{-1}(z,p_e)}.$

$\zeta$, $\hat{v}$ and $\hat{M}$ are the respective estimates of $z$, $v$ and $M$; $\Omega(D)$ and $g(D, \xi, \omega)$ are given in (A.3b) and (A.3c). Subtract the reactor model (B.2) from its estimator (B.3) to obtain the estimation error dynamics:

$$e(t_{i+1}) = A(D, \xi, \omega)e(t_i) + \int_{t_i}^{t_{i+1}} .\Omega(t_{i+1} - \tau)\pi\,q(e(\tau), e_\alpha(\tau), e_p, z(\tau), \alpha(\tau), p_e)d\tau \tag{B.4a}$$

$$e_v(t_i) = \delta e(t_i), \qquad e_M(t_i) = q_M(e(t_i), e_p, e_{p_\eta}, z(t_i), p_e, p_\eta) \tag{B.4b}$$

where

$e = \zeta - z, \quad e_v = \hat{v} - v, \quad e_M = \hat{M} - M, \quad e_p = \hat{p}_e - p_e, \quad e_\alpha = \hat{\alpha} - \alpha, \quad A = \Omega - g\delta,$
$q(e, e_\alpha, e_p, z, \alpha, p_e) = \varphi(\zeta = z + e, \hat{\alpha} = \alpha + e_\alpha, \hat{p}_e = p_e + e_p) - \varphi(z, \alpha, p_e),$
$q_M(e, e_p, e_{p_\eta}, z, p_e, p_\eta) = \eta^*(\zeta = z + e, \hat{p}_e = p_e + e_p, \hat{p}_\eta = p_\eta + e_{p_\eta}) - \eta^*(z, p_e, p_\eta).$

Consider the following bounds (on the basis of the stability of matrix $A$ and from the continuous differentiability of maps $r$, $\mu$, and $\eta$):

$$|(A(D, \xi, \omega))^i| \le a_o(\xi)(\gamma_o(D, \omega))^i,$$
$$a_o > 0, \quad 0 < \gamma_o < 1, \quad \partial_{D\,\text{or}\,\omega}\gamma_o < 0, \tag{B.5a}$$

$$|q(e, e_\alpha, e_p, z, \alpha, p_e)| \le l^q_e|e| + l^q_\alpha|e_\alpha| + l^q_p|e_p|, \tag{B.5b}$$

$$|q_M(e, e_p, e_{p_\eta}, z, p_e, p_\eta)| \le l^m_e|e| + l^m_p|e_p| + l^m_\eta|e_{p_\eta}|, \tag{B.5c}$$

$$|e_\alpha| = |\alpha| \le \varepsilon_\alpha, \qquad |e_p| \le \varepsilon_p, \qquad |e_{p_\eta}| \le \varepsilon_\eta. \tag{B.5d}$$

and apply them to the estimation error dynamics via a majorization procedure (as in [12]), to conclude that the error sequences $e(t_i)$,

$e_v(t_i)$, $e_M(t_i)$ are bounded as follows:

$$|e(t_i)| \le \sigma(t = t_i), \qquad |e_v(t_i)| \le \sigma(t = t_i),$$
$$|e_M(t_i)| \le l_e^m \sigma(t = t_i) + l_p^m \varepsilon_p + l_\eta^m \varepsilon_\eta. \tag{B.6a}$$

where

$$\dot{\sigma} = -l\sigma + \rho(l_\alpha^q \varepsilon_\alpha + l_p^q \varepsilon_p), \qquad \sigma(t_0) = a_o|e(t_0)|, \tag{B.6b}$$

$$l = D^{-1}\ln(\gamma_e), \qquad \gamma_e = \gamma_o e^{Dl_e^q \rho}, \qquad \rho = a_o e^D \gamma_o^{-1} \tag{B.6c}$$

Then, the stability condition for the dynamics (B.6b) is given by

$l > 0$ or equivalently by $\ln(\gamma_e) > 0$

This condition settles down the convergence of present-time estimates. Rewrite the stability condition as follows (for simplicity, $l_e^q$ is rewritten as $L$):

$$F(s) = s - b(a, D)e^s > 0, \quad s = -\ln(\gamma_o(D, \omega)), b(a, D) = aDe^D,$$
$$a = a_o L \tag{B.7}$$

Through the derivation of $F(s)$, obtain that:

$$s^* = -\ln(b(a, D)) \tag{B.8}$$

maximizes the function $F(s)$ if

$$b(a, D)e < 1; \tag{B.9}$$

since $a$ is a parameter, this expression sets an upper sampling time limit $D^+$ in such a way that:

$$b(a, D^+) = e^{-1}, \quad \text{or} \quad D^+ = b^{-1}(a, e^{-1}) \tag{B.10}$$

Moreover, notice that function $b$ (B.7) is directly proportional to $a$, meaning that its inverse (B.10) decreases with $a$. The above is equivalent to the first convergence condition stated in Section 4.3 for the present-time estimates.

Rewrite the equality version of inequality (B.7):

$$F(s) = s - b(a, D)e^s = 0$$

Provided $D < D^+$, this equation has two solutions: $s^- < s^*$ and $s^+ > s^*$, implying the existence of a nonempty set $(s^-, s^+)$ where $s$ can take values that fulfill the stability condition given by (B.7). Next, recalling the $s$–$\omega$ relationship (B.7), the above is equivalent to saying that there is a set $(\omega^-, \omega^+)$ where the tuning parameter $\omega$ can take values (provided $D < D^+$) to obtain convergent present-time estimates; and this is the second convergence condition stated in Section 4.3 for the present-time estimates.

On the other hand, it can be observed in (B.6) that:

(i) the present-time estimation error sequence of the reactor states (i.e., $c$, $k$ and v via $e$) and viscosity ($v$) decay exponentially with an adjustable rate (i.e., via $\gamma_o$), and with an ultimate bounded offset whose size depends on the parametric errors ($\varepsilon_p$) and on the error arisen from assuming that $\hat{\alpha} = 0$.
(ii) the present-time estimation error sequence of $M$ decays similarly to $v$ with an amplified (i.e., via $l_e^m$) and additional (i.e., via $l_p^m \varepsilon_p + l_\eta^m \varepsilon_\eta$) offset.

## Appendix C. Proof for convergence conditions of time-ahead predictions

Subtract the augmented reactor model (4a)-(4c) and (4f) from the estimator part that yields time-ahead predictions (12d) and (12e) to obtain the prediction error dynamics,

$$\dot{e}_c = r^*[e_c, e_k, e_{c_e}, c(t), k(t), c_e], \qquad e_c(t_i) = e_i^c, \qquad e_c = \hat{c} - c \tag{C.1a}$$

$$\dot{e}_k = e_v, \qquad e_k(t_i) = e_i^k, \qquad e_k = \hat{k} - k \tag{C.1b}$$
$$\dot{e}_v = -\alpha(t), \qquad e_v(t_i) = e_i^v, \qquad e_v = \hat{v} - v \tag{C.1c}$$
$$e_v(t) = \mu^*[e_c(t), e_{p_\mu}, c(t), p_\mu], \qquad e_v = \hat{v} - v \tag{C.1d}$$
$$e_m(t) = \eta^*[e_c(t), e_{p_\eta}, c(t), \rho_\eta], \qquad e_m = \hat{m} - m \tag{C.1e}$$

where

$$r^*(e_c, e_k, e_{c_e}, c, k, c_e) = r(\hat{c} = c + e_c, \hat{k} = k + e_k, \hat{c}_e = c_e + e_{c_e}) - r(c, k, c_e)$$

$$\mu^*(e_c, e_{p_\mu}, c, p_\mu) = \mu(\hat{c} = c + e_c, \hat{p}_\mu = p_\mu + e_{p_\mu}) - \mu(c, p_\mu)$$

$$\eta^*(e_c, e_{p_\eta}, c, p_\eta) = \eta(\hat{c} = c + e_c, \hat{p}_\eta = p_\eta + e_{p_\eta}) - \eta(c, p_\eta)$$

The convergence of the reactor state prediction is proved by establishing the stability of the prediction error dynamics (C.1) by means of the indirect (linearization) Lyapunov method [17]. Then, linearize the differential equation (C.1a) about $(e_c, e_k, e_{c_e})' = (0, 0, 0)'$, and hold the other equations,

$$\dot{e}_c = r_c^*(t)e_c + r_k^*(t)e_k + r_{c_e}^*(t)e_{c_e}, \qquad e_c(t_i) = e_i^c, \qquad t \in [t_i, t_F^*) \tag{C.2a}$$

$$\dot{e}_k = e_v, \qquad e_k(t_i) = e_i^k, \tag{C.2b}$$
$$\dot{e}_v = -\alpha(t), \qquad e_v(t_i) = e_i^v, \tag{C.2c}$$
$$e_v(t) = \mu^*[e_c(t), e_{p_\mu}, c(t), p_\mu], \tag{C.2d}$$
$$e_m(t) = \eta^*[e_c(t), e_{p_\eta}, c(t), p_\eta], \tag{C.2e}$$

where

$$r_c^*(t) = \partial_{e_c} r^*[c(t), k(t), c_e] = \partial_c r[c(t), k(t), c_e] = -k(t)[c_e - c(t)][c_e + 2 - 3c(t)], \quad r_c^*(t) < 0 \tag{C.3a}$$

$$r_k^*(t) = \partial_{e_k} r^*[c(t), k(t), c_e] = \partial_k r[c(t), c_e] = [1 - c(t)][c_e - c(t)]^2, \quad r_k^*(t) > 0 \tag{C.3b}$$

$$r_{c_e}^*(t) = \partial_{c_{ce}} r^*[c(t), k(t), c_e] = \partial_{c_e} r[c(t), k(t), c_e] = 2k(t)[1 - c(t)][c_e - c(t)], \quad r_{c_e}^*(t) > 0 \tag{C.3c}$$

and

$$|r_c^*(t)| \le c_e(c_e + 2)k(t), \quad 0 < r_k^*(t) < c_e^2, \quad 0 < r_{c_e}^*(t) < 2c_e k(t);$$
$$|r_c^*(t)| > r_k^*(t), \quad |r_c^*(t)| > r_{c_e}^*(t) \tag{C.3d}$$

Integrate from $t_i$ to $t = t_i + \tau$

$$e_c(t) = \beta(t, t_i)e_i^c + \int_{t_i}^{t} .\beta(t, \sigma)r_k^*(\sigma)\left[e_i^k + e_i^v(\sigma - t_i) + \int_{t_i}^{\sigma} \cdot \int_{t_i}^{s} \cdot -\alpha(s)ds\,dz\right]d\sigma + \int_{t_i}^{t} .\beta(t, \sigma)r_{c_e}^*(\sigma)e_{c_e}d\sigma \tag{C.4a}$$

$$e_k(t) = e_i^k + e_i^v(\sigma - t_i) + \int_{t_i}^{t} . \int_{t_i}^{\sigma} . -\alpha(s)ds\,d\sigma \quad t \in [t_i, t_F^*) \tag{C.4b}$$

$$e_v(t) = e_i^v + \int_{t_i}^{t} . -\alpha(\sigma)d\sigma \tag{C.4c}$$

$$e_v(t) = \mu^*[e_c(t), e_{p_\mu}, c(t), p_\mu], \tag{C.4d}$$
$$e_m(t) = \eta^*[e_c(t), e_{p_\eta}, c(t), p_\eta], \tag{C.4e}$$

where

$$\beta(t, t_i) = \exp\left[\int_{t_i}^{t} .r_c^*(\sigma)d\sigma,\right] \tag{C.5}$$

Notice the $\beta$ function is decreasing because of $r_c^*(t) < 0$. Take norms, taking into account that:

$$|\beta(t, t_i)| = \exp\left[\int_{t_i}^{t} .r_c^*(\sigma)d\sigma\right] \leq e^{-\lambda(t,t_i)}, \quad |\alpha(t)| \leq \varepsilon_\alpha, \quad |e_{c_e}| \leq \varepsilon_c, \tag{C.6a}$$

$$|\mu^*(e_c, e_{p_\mu}, c, p_\mu)| \leq l_c^\mu |e_c| + l_\mu \varepsilon_\mu, \qquad \varepsilon_\mu = |\hat{p}_\mu - p_\mu|, \tag{C.6b}$$

$$|\eta^*(e_c, e_{p\eta}, c, p_\eta)| \leq l_c^\eta |e_c| + l_\eta \varepsilon_\eta, \qquad \varepsilon_\eta = |\hat{p}_\eta - p_\eta|, \tag{C.6c}$$

and obtain that the prediction error motions are bounded as follows:

$$|e_c(t)| \leq e^{-\lambda(t,t_i)}|e_i^c| + \int_{t_i}^{t} .e^{-\lambda(t,\sigma)}|r_k^*(\sigma)|\left[|e_i^k| + |e_i^\nu|(\sigma - t_i) + (1/2)\varepsilon_\alpha(\sigma - t_i)^2\right] d\sigma + \int_{t_i}^{t} .e^{-\lambda(t,\sigma)}|r_{c_e}^*(\sigma)|\varepsilon_c d\sigma \tag{C.7a}$$

$$|e_k(t)| \leq |e_i^k| + e_i^{\mathrm{v}}|(t - t_i) + (1/2)\varepsilon_\alpha(t - t_i)^2, \quad t \in [t_i, t_F^*) \tag{C.7b}$$

$$|e_{\mathrm{v}}(t)| \leq |e_i^{\mathrm{v}}| + \varepsilon_\alpha(t - t_i), \tag{C.7c}$$

$$|e_\nu(t)| \leq l_c^\mu |e_c(t)| + l_\mu \varepsilon_\mu, \tag{C.7d}$$

$$|e_m(t)| \leq l_c^\eta e_c(t)| + l_\eta \varepsilon_\eta, \tag{C.7e}$$

Then, it can be observed that:

(i) From inequalities (C.7b) and (C.7c), the prediction error motion corresponding to the $k$ and $\nu$ states is growing with time. However, since the batch time is finite ($t_F^*$), and assuming that the present-time estimation errors of $k$ and $\nu$ ($e_i^k, e_i^\nu$) are sufficiently small (or the present-time state estimates are convergent), it can be observed that the prediction error will be bounded as follows:

$$|e_k(t)| \leq \varepsilon_k(t_F^* - t_i),$$
$$\varepsilon_k(t_F^* - t_i) = |e_i^k| + |e_i^{\mathrm{v}}|(t_F^* - t_i) + (1/2)\varepsilon_\alpha(t_F^* - t_i)^2, \quad t_i \leq t \leq t_F^* \tag{C.8a}$$

$$|e_{\mathrm{v}}(t)| \leq \varepsilon_k(t_F^* - t_i), \qquad \varepsilon_k(t_F^* - t_i) = |e_i^{\mathrm{v}}| + \varepsilon_\alpha(t_F^* - t_i) \tag{C.8b}$$

Consequently, it can be said that the prediction error motion will stay sufficiently close to the point $(e_k, e_{\mathrm{v}})' = (0, 0)$; concluding that the prediction error motion of $k$ and $\nu$ is *practically* stable, and therefore the $k$ and $\nu$ predictions are *practically* convergent.

(ii) From inequality (C.7a), the original nonlinear error dynamics of conversion (C.1a) is exponentially stable with a decaying rate fixed by the kinetics (i.e., via $r_c^*(t)$), and with an ultimate offset (i.e., second term on the right-hand side of (C.7a) whose size depends on the present-time estimate error of the kinetics variables (i.e., via $e_i^k$ and $e_i^{\mathrm{v}}$), the parametric errors ($\varepsilon_p$), and on the error arisen from making $\hat{\alpha} = 0$. It can be observed that the ultimate offset can grow with time, however, besides the fact that $|r_c^*(t)| > r_\kappa^*(t)$ and $|r_c^*(t)| > r_{c_e}^*(t)$, the batch time is finite; then, the second term will not surpass a certain value (see (C.8)). Invoking the Lyapunov linearization method, this property holds for the original nonlinear prediction error dynamic (C.1a) in the close vicinity of $(e_c, e_k, e_{c_e})' = (0, 0, 0)'$, and therefore the conversion prediction is convergent.

(iii) From (C.7c) and (C.7d), since the prediction error motion is decreasing with an ultimate bounded offset, the viscosity and AMW prediction errors are decreasing in the same way as the conversion one, but with an amplified offset due to parametric errors (i.e., via $l_c^\mu$, $l_\mu\varepsilon_\mu$, $l_c^\eta$, and $l_\eta\varepsilon_\eta$).

## References


[1] R. Rosas, Modelamiento de un reactor de alquidales, Master Thesis, Universidad Autónoma Metropolitana–Iztapalapa, México, 2001.
[2] J.R. Richards, J.P. Congalidis, Measurement and control of polymerization reactors, Comput. Chem. Eng. 30 (2006) 1447–1463.
[3] P.J. Flory, Principles of Polymer Chemistry, Cornell Univ. Press, New York, 1953.
[4] C.C. Lin, K.H. Hsieh, The kinetics of polyesterification. I. Adipic acid and ethylen glycol, J. Appl. Polym. Sci. 21 (1977) 2711–2719.
[5] A.I. Aigbodion, F.E. Okieimen, Kinetics of the preparation of rubber seed oil alkyds, Eur. Polym. J. 32 (1996) 1105–1108.
[6] J. Alvarez, P. Gonzalez, Constructive control of polymerization reactors, J. Process Control. 17 (2007) 463–476.
[7] M. Soroush, C. Kravaris, Multivariable nonlinear control of a continuous polymerization reactor: an experimental study, AIChE J. 39 (1993) 1920–1937.
[8] R.K. Mutha, W.R. Cluett, A. Penlidis, On-line nonlinear model-based estimation and control of a polymer reactor, AIChE J. 43 (1997) 3042–3058.
[9] C.M. Astorga, N. Othman, S. Othman, H. Hammouri, T.F. McKenna, Nonlinear continuous-discrete observer application to emulsion polymerization reactors, Control Eng. Pract. 10 (2002) 3–13.
[10] H. Schuler, C.U. Schmidt, Calorimetric-state estimators for chemical reactor diagnosis and control: review of methods and applications, Chem. Eng. Sci. 47 (1992) 899–913.
[11] F. López-Serrano, J.E. Puig, J. Alvarez, On the modeling assessment of thermal styrene polymerization, AIChE J. 50 (2004) 2246–2257.
[12] H. Hernandez, J. Alvarez, Robust estimation of continuous nonlinear plants with discrete measurements, J. Process Control. 13 (2003) 69–89.
[13] T. López, H. Hernández, J. Alvarez, Robust nonlinear estimation of alkyd reactors with discrete-delayed measures, in: Proc. ADCHEM (IFAC) Symp., Pisa, Italy, 2000, pp. 359–364.
[14] H. Fujita, A. Kishimoto, Interpretation of viscosity data for concentrated polymer solutions, J. Chem. Phys. 34 (1961) 393–398.
[15] T.C. Patton, Alkyd Resin Technology, John Wiley & Sons, New York, 1962.
[16] J.J. D'Azzo, C.H. Houpis, S.N. Sheldon, Linear Control System Analysis and Design: Conventional and Modern, fourth ed., McGraw-Hill, 1995.
[17] J.J.E. Slotine, W. Li, Applied Nonlinear Control, Prentice Hall, 1991.